

Untwisting the Boerdijk-Coxeter Helix

Robert L. Read read.robert@gmail.com

Abstract. The Boerdijk-Coxeter helix (BC helix, or tetrahelix) is a face-to-face stack of regular tetrahedra forming a helical column. Considering the edges of these tetrahedra as structural members, the resulting structure is attractive and inherently rigid, and therefore interesting to architects, mechanical engineers, and roboticists. A formula is developed that matches the visually apparent helices forming the outer rails of the BC helix. This formula is generalized to a formula convenient to designers. Formulae for computing the parameters that give edge-length minimax-optimal tetrahelices are given, defining a continuum of tetrahelices of varying curvature. The endpoints of the optimality of this continuum are the BC helix and a structure of zero curvature, the *equitetrabeam*. Numerically finding the rail angle from the equation for pitch allows optimal tetrahelices of any pitch to be designed. An interactive tool for such design and experimentation is provided: <https://pubinv.github.io/tetrahelix/>. A formula for the inradius of optimal tetrahelices is given. Utility for static and variable geometry truss/space frame design and robotics is discussed.

Key words. Boerdijk-Coxeter helix, tetrahelix, robotics, tetrobot, unconventional robots, structural engineering, mechanical engineering, tensegrity, variable-geometry truss

18 AMS subject classifications. 51M15

1. Introduction. The Boerdijk-Coxeter helix[3] (BC helix) (see Figure 1 and ??, is a face-to-face stack of tetrahedra that winds about a straight axis. Because architects, structural engineers, and roboticists are inspired by and follow such regular mathematical models but can also build structures and machines of differing or even dynamically changing length, it is useful to develop the mathematics of structures formed from tetrahedra where we relax regularity.

The vertices of the tetrahedra lie upon three helices about the central axis. The Glussbot[11] (or Tetrobot)[8] uses the regularity of this geometry to make a tentacle-like robot that can crawl like a slug or mollusc. These modular robotic systems use mechanical actuators which can change their length, connected by special joints, such as the 3D printable Song-Kwon-Kim[15] joint in the case of the Glussbot, or the CMS joint[7], in the case of the Tetrobot, which allow many members to meet in a single point. Such machines can follow purely regular mathematical models such as the Boerdijk-Coxeter helix or the Octet Truss[4].

32 Buckminster Fuller called the BC helix a *tetrahelix*[5], a term now commonly used. In this
 33 paper we reserve *BC helix* to mean the purely regular structure and use *tetrahelix* to refer to
 34 any structure isomorphic to the BC helix.

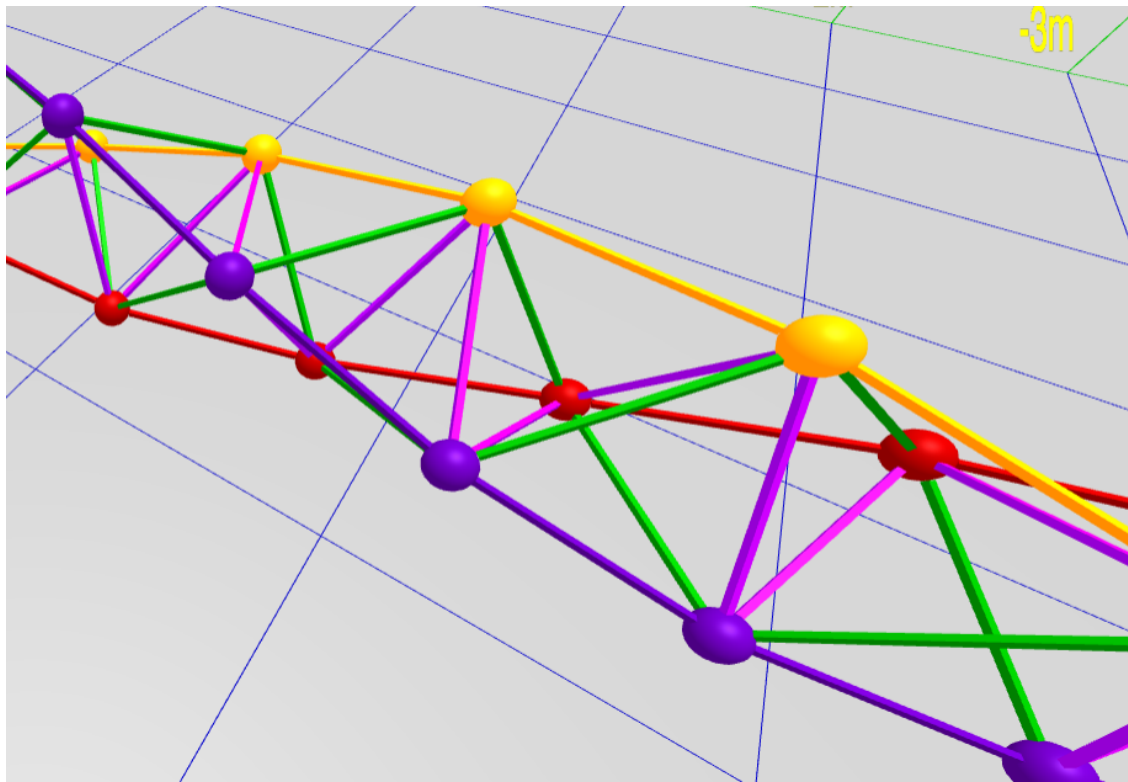


Figure 1. BC Helix Close-up (partly along axis)

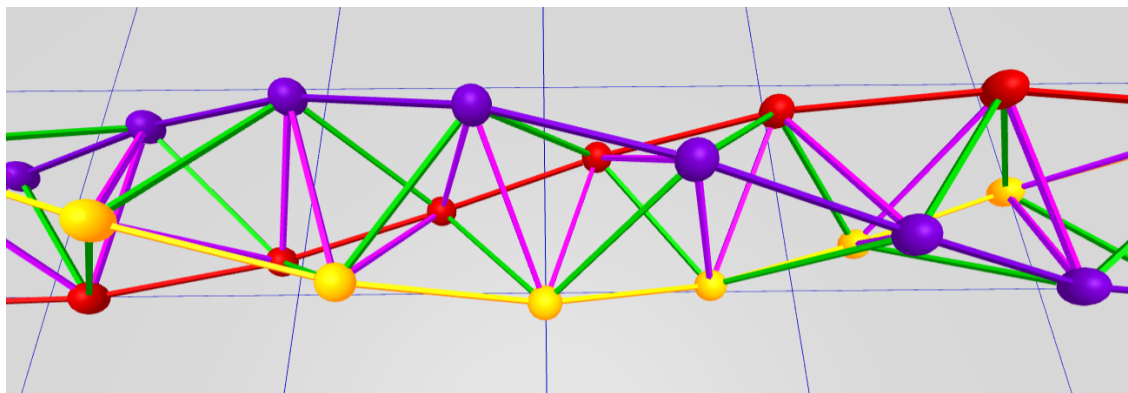


Figure 2. BC Helix Close-up (orthogonal)

35 Imagining Figures 1 and 2 as a static mechanical structure, we observe that it is useful
 36 to the mechanical engineer or roboticist because the structure remains an inherently rigid,
 37 omni-triangulated space frame, which is mechanically strong. Then we can imagine that each
 38 static edge is replaced with an actuator that can dynamically become shorter or longer in
 39 response to electronic control, and the vertices are a joint that supported sufficient angular

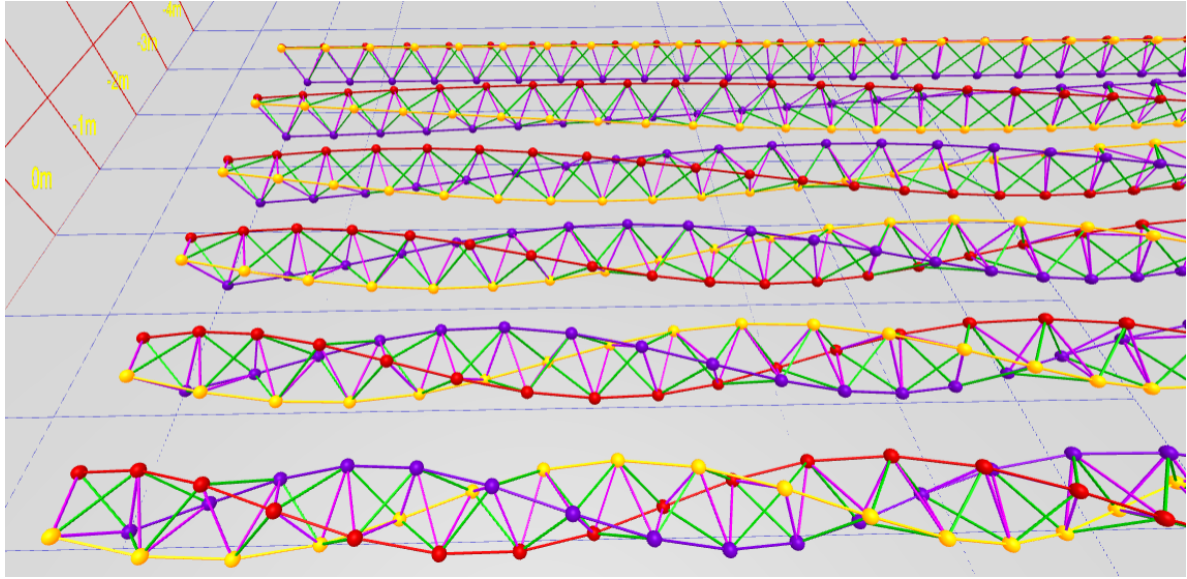


Figure 3. A Continuum of Tetrahelices

40 displacement for this to be possible. An example of such a machine is a glussbot, shown in
41 [Figure 12](#).

42 A BC helix does not rest stably on a plane. It is convenient to be able to “untwist” it and
43 to form a tetrahelix space frame that has a flat planar surface. By making length changes in a
44 certain way, we can untwist a tetrahelix to form a *tetrabeam* which has planar faces and has,
45 for example, an equilateral triangular profile. This paper develops the equations needed to
46 untwist the tetrahelix. All math developed here is available in JavaScript and demonstrated by
47 an interactive design website <https://pubinv.github.io/tetrahelix/>[12], from which Figures 1
48 to 3 are taken.

49 Figure 3 displays a continuum of tetrahelices optimal in a certain sense, which is the main
50 result of this paper. The closest helix is the BC helix, and the furthest is the equitetrabeam,
51 defined in [section 6](#) and [Figure 7](#) and ??.

52 **2. A Designer’s Formulation of the BC Helix.** We would like to design nearly regular
53 tetrahelices with a formula that gives the vertices in space. Eventually we would like to design
54 them by choosing the lengths of a small set of members. In a space frame, this is a static
55 design choice; in a tetrobot, it is a dynamic choice that can be used to twist the robot and/or
56 exert linear or angular force on the environment.

57 Ideally we would have a simple formula for defining the nodes based on any curvature or
58 pitch we choose. It is a goal of this paper to relate the Cartesian coordinate approach and
59 the member-length approachx to generating a tetrahelix continuum.

60 H.S.M Coxeter constructs the BC helix[3] as a repeated rotation and translation of the
61 tetrahedra, showing the rotation is:

$$62 \quad \theta_{bc} = \arccos(-2/3)$$

63 and the translation:

$$64 \quad h_{bc} = 1/\sqrt{10}$$

65 θ_{bc} is approximately $0.37 \cdot 2\pi$ radians or 131.81 degrees. The angle θ_{bc} is the rotation of
66 each tetrahedron, not the tetrahedra along a rail. In [Figure 1](#), each tetrahedron has either a
67 yellow, blue, or red outer edge or rail. That is, a blue-rail tetrahedron is rotated slightly more
68 than a $1/3$ of a revolution to match the face of the yellow tetrahedra.

69 R.W. Gray's website[\[6\]](#), repeating a formula by Coxeter[\[3\]](#) in more accessible form, gives

70 the Cartesian coordinates $\begin{bmatrix} x \\ y \\ z \end{bmatrix}$ for a counter-clockwise BC Helix in a right-handed coordinate
71 system:

$$72 \quad (1) \quad \mathbf{V}(n) = \begin{bmatrix} r_{bc} \cos n\theta_{bc} \\ r_{bc} \sin n\theta_{bc} \\ nh_{bc} \end{bmatrix}, \text{ where: } \begin{aligned} r_{bc} &= \frac{3\sqrt{3}}{10} \approx 0.5196 \\ h_{bc} &= 1/\sqrt{10} \approx 0.3162 \\ \theta_{bc} &= \arccos(-2/3) \end{aligned}$$

73 where n represents each integer numbered node in succession on every colored rail.

74 The apparent rotation of a vertex on an outer-edge, that is $\mathbf{V}(n)$ relative from $\mathbf{V}(n+3)$
75 for any integer n in (1), is $3\theta_{bc} - 2\pi$.

76 This formula defines a helix, but it is not any of the apparent helices, or *rail* helices, of the
77 BC helix, but rather one that winds three times as rapidly through all nodes. To a designer of
78 tetrahelices, it is more natural to think of the three helices which are visually apparent, that
79 is, those three which are closely approximated by the outer edges or rails of the BC helix. We
80 think of each of these three rails as being a different color: red, blue, or yellow. This situation
81 is illustrated in [Figure 4](#), wherein the black helix represents that generated by (1), and the
82 colored helices are generated by (2).

83 In order to develop the continuum of slightly irregular tetrahelices described in [section 7](#),
84 we need a formula that gives us the nodes of just one rail helix, denoted by color c and integer
85 node number n :

$$86 \quad (\forall n \in \mathbb{Z}, \forall c \in \{0, 1, 2\} : \mathbf{H}_{BCcolored}(n, c) = \mathbf{V}(3n + c))$$

87 Such a helix can be written:

$$88 \quad (2) \quad \mathbf{H}_{BCcolored}(n, c) = \begin{bmatrix} r_{bc} \cos ((3\theta_{bc} - 2\pi)n + c\theta_{bc}) \\ r_{bc} \sin ((3\theta_{bc} - 2\pi)n + c\theta_{bc}) \\ 3h_{bc}(n + c/3) \end{bmatrix}, \text{ where } \begin{aligned} r_{bc} &= \frac{3\sqrt{3}}{10} \\ h_{bc} &= 1/\sqrt{10} \\ \theta_{bc} &= \arccos(-2/3) \end{aligned}$$

89 In this formula, integral values of n may be taken as a node number for one rail and
90 used to compute its Cartesian coordinates. Allowing n to take non-integer values defines a
91 continuous helix in space which is close to the segmented polyline of the outer tetrahedra
92 edges, and equals them at integer values.

93 [Figure 4](#) illustrates this difference with a 7-tetrahedra BC helix, which is in fact the same
94 geometry as the robot illustrated in [Figure 12](#). Although the nodes coincide, (1) evaluated
95 at real values generates the black helix which runs through every node, and (2) defines the

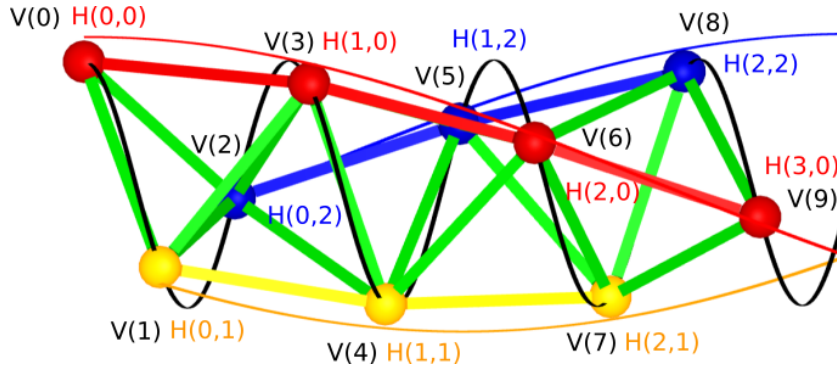


Figure 4. Rail helices (H) vs. Coxeter/Gray helix (V)

96 red, yellow, and blue helices. (In this figure these rail helices have been rendered at a slightly
97 higher radius than the nodes for clarity; in actuality the maximum distance between the
98 continuous, curved helix and the straight edges between nodes is much smaller than can be
99 clearly rendered.)

100 The quantity $(3\theta_{bc} - 2\pi) \approx 35.43^\circ$ is the angular shift between $\mathbf{V}(3n+c) = \mathbf{H}_{BCcolored}(n, c)$
101 and $\mathbf{V}(3(n+1)+c) = \mathbf{H}_{BCcolored}(n+1, c)$. This quantity appears so often that we call it the
102 “rail angle ρ ”. For the BC helix, $\rho_{bc} = (3\theta_{bc} - 2\pi)$.

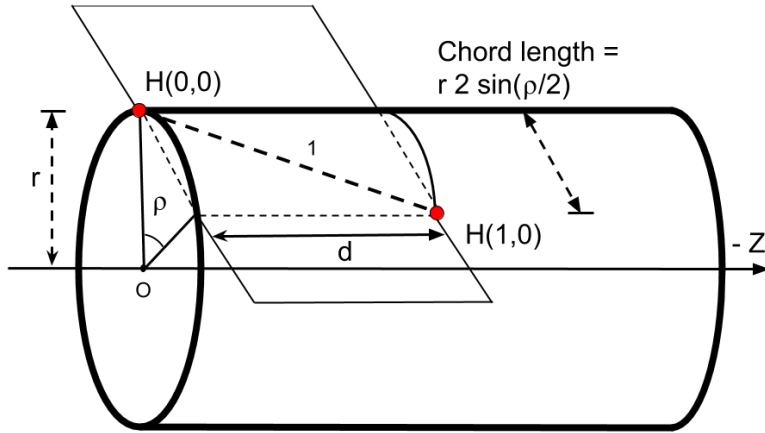


Figure 5. Rail Angle Geometry

103 Note in Figure 5 the z -axis travel for one rail edge is denoted by d . In (1) and (2),
104 the variable h is used for one third of the distance we name d . We will later justify that
105 $d = 3h$. In this paper we assume the length of a rail is always 1 as a simplification, except in

106 proofs concerning rail length. (We make the rail length a parameter in our JavaScript code
 107 in https://github.com/PubInv/tetrahelix/blob/master/js/tetrahelix_math.js [12].)

108 The $\mathbf{H}_{BC\text{colored}}(n, c)$ formulation can be further clarified by rewriting directly in terms of
 109 the rail angle ρ_{bc} rather than θ_{bc} . Intuitively we seek an expression where $c/3$ is multiplied by
 110 a $1/3$ rotation plus the rail angle ρ . We expand the expressions θ_{bc} and ρ_{bc} in (2) and seek to
 111 isolate the term $c2\pi/3$.

$$\begin{aligned} 112 \quad c\theta_{bc} &= \{\text{we aim for } 3 \text{ in denominator, so we split...}\} \\ 113 \quad (c/3)(3\theta_{bc}) &= \{\text{we want } 2\pi \text{ in numerator, so add canceling terms...}\} \\ 114 \quad (c/3)((3\theta_{bc} - 2\pi) + 2\pi) &= \{\text{definition of } \rho_{bc}\}... \\ 115 \quad (c/3)\rho_{bc} + c2\pi/3 &= \{\text{algebra...}\} \\ 116 \quad c(\rho_{bc} + 2\pi)/3 & \\ 117 \end{aligned}$$

119 This allows us to redefine:

$$120 \quad (3) \quad \mathbf{H}_{BC\text{colored}}(n, c) = \begin{bmatrix} r \cos \rho_{bc} n + c(\rho_{bc} + 2\pi)/3 \\ r \sin \rho_{bc} n + c(\rho_{bc} + 2\pi)/3 \\ (n + c/3)h_{bc} \end{bmatrix}, \text{ where } \begin{aligned} \rho_{bc} &= (3\theta_{bc} - 2\pi) \\ h_{bc} &= 1/\sqrt{10} \end{aligned}$$

121 Recall that $c \in \{0, 1, 2\}$, but n is continuous (rational or real-valued.) We can now assert
 122 that in Figure 4 the black helix winds at $\frac{3\theta_{bc}}{\rho_{bc}} \approx 11.16$ times the rate of a rail helix.

123 From this formulation it is easy to see that moving one vertex on a rail ($\mathbf{H}_{BC\text{colored}}(n, c)$)
 124 to $\mathbf{H}_{BC\text{colored}}(n + 1, c)$ for any n and c) moves us ρ_{bc} radians around a circle. Since:

$$125 \quad \frac{2\pi}{\rho_{bc}} \approx 10.16$$

126 we can see that there are approximately 10.16 red, blue or yellow tetrahedra on one rail in a
 127 complete revolution of the tetrahelix.

128 The *pitch* of any tetrahelix, defined as the axial length of a complete revolution where
 129 $\rho \neq 0$ is:

$$130 \quad (4) \quad p(\rho) = \frac{2\pi \cdot d}{\rho}$$

131 The pitch of the Boerdijk-Coxeter helix of edge length 1 is the length of three tetrahedra
 132 times this number:

$$133 \quad \frac{3h_{bc} \cdot 2\pi}{\rho_{bc}} = \frac{6\pi}{\sqrt{10}\rho_{bc}} \approx 9.64$$

135 The pitch is less than the number of tetrahedra because the tetrahedra edges are not
 136 parallel to the axis of the tetrahelix. It is a famous and interesting result that the pitch is
 137 irrational. A BC helix never has two tetrahedra at precisely the same orientation around the

138 z -axis. However, this is inconvenient to designers, who might prefer a rational pitch. The
139 idea of developing a rational period by arranging solid tetrahedra by relaxing the face-to-
140 face matching has been explored[13]. We develop below slightly irregular edge lengths that
141 support, for example, a pitch of precisely 12 tetrahedra in one revolution which would allow an
142 architect to design a column having a basis and a capital in the same relation to the tetrahedra
143 they touch at the bottom and top of the column.

144 **3. Optimal Tetrahelices are Triple Helices.** We use the term *tetrahelix* to mean any
145 structure physically constructible of vertices and finite edges which is isomorphic to the BC
146 helix and in which the vertices lie on three helices. By isomorphic we mean there is a one-
147 to-one mapping between both vertices and edges in the two tetrahelices. One could consider
148 various definitions of optimality for a tetrahelix, but the most useful to us as roboticists
149 working with the Tetrobot concept is to minimize the maximum ratio between any two edge
150 lengths, because the Tetrobot uses mechanical linear actuators with limited range of extension.

151 A *triple helix* is three congruent helices that share an axis. We show that optimal tetra-
152 helices are in fact triple helices with the same radius, so that all vertices are on a cylinder. In
153 stages, we demonstrate that optimal tetrahelices:

- 154 1. have the same pitch,
- 155 2. have parallel axes,
- 156 3. share the same axis,
- 157 4. have the same radius,
- 158 5. have the same rail lengths,
- 159 6. have axially equidistant nodes, and therefore
- 160 7. are in fact triple helices.

161 Suppose that all three rails do not have the same pitch. Starting at any shortest edge
162 between two rails, as we move from node to node away from our start edge the edge lengths
163 between rails must always lengthen without bound, which cannot be optimal. So we are
164 justified in talking about the *pitch* of the optimal tetrahelix as the pitch of its three rail
165 helices, even though there are three such helices of equivalent pitch.

166 Similarly, if the axes are not parallel, there is an edge of unbounded length in the structure,
167 so we do not consider such cases.

168 Define a *minimax edge-length optimal tetrahelix* or just an *optimal tetrahelix* to be a
169 tetrahelix for which there exists no other tetrahelix with lower ratio of longest edge length to
170 shortest edge length.

171 We wish to show that in an optimal tetrahelix, all vertices lie on the cylinder of radius r ,
172 regardless of where they lie on the z -axis.

173 As a little lemma for the proof below, observe that a tetrahelix of zero radius, where all
174 points lie on the same line, is not as optimal as a tetrahelix of a small radius. The edges
175 between rails will be shorter than the rail edges, and moving them apart slightly lengthens
176 the between-edge rails, improving the ratios.

177 In the proof below we find useful to consider projection diagrams that are the axial pro-
178 jection of a tetrahelix onto the XY -plane. [Figure 10](#) is an example of such a diagram.

179 **Lemma 1.** *If the rail angle $0 < \rho < \pi$ is a rational multiple of π , then the projection of
180 edges long a helix of that rail angle along the z -axis onto the XY -plane form a regular polygon*

181 of 3 or more sides, else they fill in a complete circle.

182 *Proof.* All points lying on a helix projected along the axis lie on a circle in the XY -plane.
183 Helices are periodic in the z dimension modulo 2π . If $2\pi/\rho$ is irrational, the projection onto
184 the XY -plane will contain an unbounded number of points on a circle. If and only if $2\pi/\rho$
185 is rational, the projection onto the XY -plane will contain a finite number of points. Because
186 π is transcendental and irrational, $2\pi/\rho$ is rational if and only $\rho = a\pi/b$, where a and b are
187 integers. Since $\rho < \pi$, $a < b$, and since $\rho > 0$, $a > 0$. The number of points in the projection
188 is $2b$ if a is odd, and b if a is even. This polygon has at least 3 sides, since either either ρ is
189 irrational or $b > a$, and therefore $b \geq 2$. If $a/b = 1/2$, the projection is a square, which has
190 four sides. ■

191 **Theorem 2.** Any optimal tetrahelix with a rail angle of magnitude less than π has all three
192 axes conincident.

193 *Proof.* Case 1: Suppose that ρ is zero. Each helix has zero curvature, that is, is a straight
194 line. These lines are equivalent to some three degenerate helices, possibly with different radii,
195 so long as there is a phase term in the defintion of the helix, as in (2). We later show the radii
196 must be equivalent.

197 Case 2: Suppose that ρ is positive but less than π . In this case each rail helix has
198 curavature. The projection of points in the XY plane creates a figure guaranteed to have
199 points on either side of any line through the axis of such a helix, because the figure is either
200 an n -gon or a circle Lemma 1. We show that the three helices share a common axis.

201 Without loss of generality define the Red helix to have its axis on the z -axis. Since either
202 a Red-to-Yellow or a Red-to-Blue edge is either a minimum or a maximum, without loss of
203 generatlity define the Blue helix to be a helix that has an edge connection to the Red helix
204 that is either a maximum or a minimum. Let B' be a translation in the XY -plane of the
205 blue helix B so that its axis is the z -axis and conincident with the red helix R . Let D be the
206 distance between the axis of the Blue helix B and B' . We will show that if $D > 0$ then B
207 “wobbles” in a way that cannot be optimal. Define a wobble vector by:

208
$$\mathbf{W}(n) = \mathbf{B}(n) - \mathbf{B}'(n)$$

209 where $\mathbf{B}(n)$ and $\mathbf{B}'(n)$ is the cartesian vector $\begin{bmatrix} x \\ y \end{bmatrix}$ for the projection of the n th vertex of B
210 and B' . Note that $\|\mathbf{R}(n) - \mathbf{B}'(n+k)\|$ (the Euclidean distance of the vertices) is a constant
211 for any k , because R and B' have the same pitch and the same axis, even if they do not have
212 the same radius.

213 Figure 6 illustrates this situation. Like most diagrams, it is over specific, in that the two
214 circles are drawn of the same radius but we do not depend upon that in this proof. The
215 diagram represents the projection along the z axis of a few points into the XY -plane.

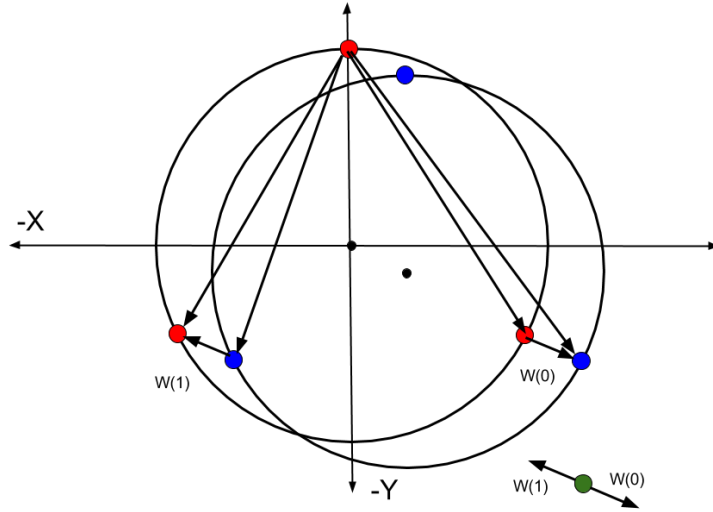


Figure 6. Wobble Vectors from Non-Coincident Axes

216 Since $\rho < \pi$ by assumption, by [Lemma 1](#), the set of wobbles $\{\mathbf{W}(n)\}$ for any n contains
 217 at least three vectors, at least two of which pointing in different directions. For any point not
 218 at the origin, at least one of these vectors moves closer to the point and at least one moves
 219 further away.

220 The set of all lengths in the tetrahelix is a superset of: $L = \{||\mathbf{R}(n) - \mathbf{B}(n)||\}$, which
 221 by our choice has at least one longest or shortest length. (Note this is just the Euclidean
 222 distance formula written as a Euclidean norm.) $L = \{||\mathbf{R}(n) - (\mathbf{B}'(n) + \mathbf{W}(n))||\}$ and so
 223 $L = \{||(\mathbf{R}(n) - \mathbf{B}'(n)) - \mathbf{W}(n)||\}$. But $\mathbf{R}(n) - \mathbf{B}'(n)$ is a constant, so the minimax value of
 224 L is improved as $||\mathbf{W}(n)||$ decreases. By our choice that there is a Blue-to-Red edge that is
 225 either a maximum or a minimum, this improves the minimax value of the total tetrahelix.

226 This process can be carried out on both the Blue and Yellow helices (perhaps simulta-
 227 neously) until $\mathbf{W}(n)$ is zero for both, finding a tetrahelix of improved overall minimax value
 228 at each step. So a tetrahelix is optimal only when $\mathbf{W}(n) = 0$, and therefore when $D = 0$
 229 $\mathbf{B}(n) = \mathbf{B}'(n)$, and all three axes are coincident. ■

230 Now that we have show that axes are coincident and parallel and that the pitches are
 231 the same for all helices, we can assert that any optimum tetrahelix can be generated with an
 232 equation for helices:

233 (5)
$$\mathbf{V}_{\text{triple}}(n, c) = \begin{bmatrix} r_c \cos(n\alpha + c2\pi/3 + \phi_c) \\ r_c \sin(n\alpha + c2\pi/3 + \phi_c) \\ \frac{d(n+c/3)}{3} \end{bmatrix}, \text{ where: } c \in \{0, 1, 2\}$$

234 which would be much more complicated if the axes were not coincident. Note that we have
 235 not yet show that the relationships of the radius r_c or the phase ϕ_c for the three helices, so we

denoted them with a c subscript to show they are dependent on the color. We have not yet investigated in the general case the relationships between α , r , ϕ and d in (5). In section 4 we give a more specific version of this formula which generates optimal tetrahelices. We observe that when $\alpha = 0$, the helices are degenerate, having curvature of 0, but because of the ϕ_c term, they are not collinear.

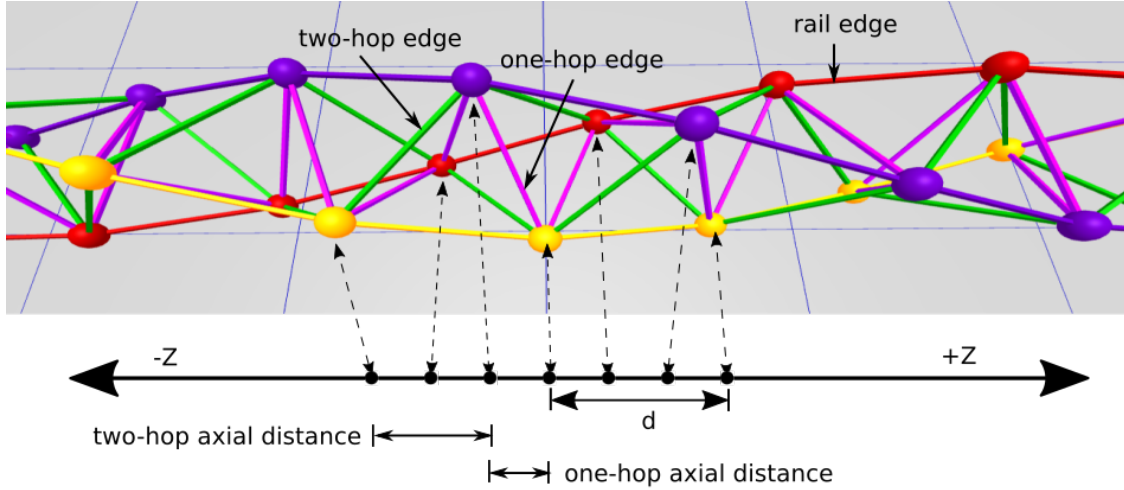


Figure 7. Edge Naming

In principle in any three helices generated with (5) has at most nine distinct edge length classes. Each edge that connects two rails potentially has a longer length and shorter length we denote with a + or -. So the classes are $\{RR, BB, YY, RB_+, RB_-, BY_+, BY_-, RY_+, RY_-\}$. If when projecting all vertices onto the z -axis (dropping the x and y coordinates), the interval defined by the z axis value of its endpoints contains no other vertices, we call it a *one-hop* edge, and if it does contain another vertex we call it a *two-hop* edge, as illustrated in Figure 7. Then there are 3 rail edges $\{RR, BB, YY\}$, 3 one-hop lengths $\{RB_-, BY_-, RY_-\}$ between each pair of 3 rails, and 3 two-hop lengths $\{RB_+, BY_+, RY_+\}$ between each pair of 3 rails, where the two-hop length is at least the one-hop length. However, if we generate the three helices symmetrically with (5), many of these lengths will be the same. In fact, it is possible that there will be only two distinct such classes (or even one, in the purely regular BC helix.)

Theorem 3. *Optimal tetrahelices have the same radii for all three helices.*

Proof. To prove this we exhibit a symmetric tetrahelix (not yet shown to be optimal) which happens to be a triple helix, that has the property that all rail edges are equal to all one-hop edges and all two-hop edges are equal to each other. Observe that although we have not yet given the formula for the radii of such a triple helix, we observe there are some values for r and α , and ϕ in (5) for which all the three helices are symmetrically and evenly spaced. Furthermore, we can choose these values such that the three rail edges are of length unity and so that the one-hop lengths are also all of length unity, and the two-hop lengths are slightly longer. We call such a tetrahelix a two-class tetrahelix.

Now consider a tetrahelix in which the radius of one of the helices is different. By the connections made in a tetrahelix, any increase to a radius increases both a one-hop and two-hop distance, and any decrease likewise decreases two. Since there exists a tetrahelix which has only two distinct classes of edge lengths, (the smaller being one-hop = rail, the larger being the two-hop distance), the helix with a larger radius increases a longest edge without increasing a shortest edges. Likewise, a helix with a smaller radius decreases a one-hop edge without decreasing a two-hop edge. Therefore, a tetrahelix with different radii is not as good as some two-class tetrahelix generated by (5), and so it not optimal. We have not yet proved that a two-class tetrahelix is optimal, but it suffices to show that there exist such a better tetrahelix to show that different radii imply a suboptimal tetrahelix. ■

Because an optimal tetrhelix has equivalent radii and equivalent pitch for all three helices, it has equivalent rail edge lengths. Likewise, there is a single rail angle ρ that represents the rotation of two nodes connected by a single rail edge, and it is the same for all three rails.

Now that we have shown that any optimal tetrahelix vertices are on helices of the same axes and pitch, we see that the vertices of any optimal tetrahelix will lie on a cylinder, or a circle when the axis dimension is projected out. Therefore it is reasonable to now speak of the singular *radius r* of a tetrahelix as the radius of the cylinder. We can now go on to the harder proof about where vertices occur along the z -axis.

We show that in fact the nodes must be distributed in even thirds along the z -axis, as in fact they are in the regular BC helix.

However, we have already shown the rail lengths are equal in any optimal tetrahelix.

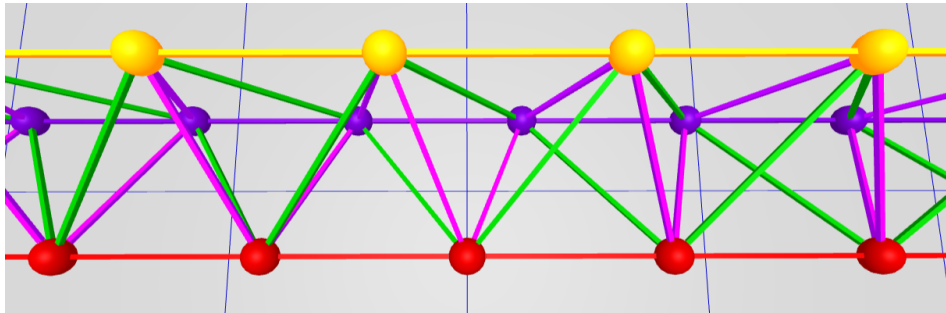


Figure 8. Equitetrabeam

Figure 8 shows the equitetrabeam, which is defined in section 6, but also conveniently illustrates the one-hop and two-hop edge definitions. The green edges are the two-hop edges and the purple edges are the one-hop edges. Note that the green edges are slightly longer than the purple edges. In Figure 7, which depicts the BC helix, the two-hop and one-hop edges are of equal length (but the projection onto the z -axis, the axial length, of the two-hop edge is longer than the axial one-hop length.)

Theorem 4. *An optimal tetrahelix of any rail angle $\rho < \pi$ is a triple helix with all vertices evenly spaced at $d/3$ intervals on the z axis. Any one tetrahedron in a tetrahelix has 1 rail edge, 2 one-hop edges connected to the rail and 2 two-hop edges connected to the rail. The sixth edge is opposite of the rail edge and is a one-hop edge.*

292 *Proof.* Consider a tetrahelix in which the vertices are evenly spaced at $d/3$ intervals on
 293 the z axis. Every edge is either a rail edge, or it makes one hop, or it makes two hops. All of
 294 the one-hop edges are equal length. All of the two-hop edges are equal length.

295 Every vertex is connected to 4 non-rail edges. There is a one-hop edge in both the positive
 296 and negative z direction. Likewise there is a two-hop edge in both the positive and negative
 297 z direction. Let A be the set of edge lengths, which has only 3 members, represented by
 298 $A = \{o, t, r\}$ for the one-hop, two-hop, and rail edge lengths.

299 Any attempt to perturb any rail in either z direction lengthens one two-hop edge to t' ,
 300 where $t' > t$ and shortens one one-hop edge $o' < o$. Let $B = \{o', t'\} \cup A$ be the edge lengths
 301 of such a perturbed tetrahelix. The minimax of B is greater than the minimax of A since
 302 there is a single rail length which cannot be both greater than t' and o' and less than t' and
 303 o' . Therefore, any optimal tetrahelix has all one-hop edges between all rails equal to each
 304 other, and all two-hop edges equal to each other, and the z distances between rails equal, and
 305 therefore $d/3$ from each other. ■

306 Note that based on [Theorem 4](#), there are only 3 possible lengths in an optimal tethrahelix,
 307 and we are justified in classifying edge lengths as *rail*, *one-hop*, or *two-hop*. The one-hop edges
 308 are the edges between rails that are closest on the z -axis, and the two-hop edges are those
 309 that skip over a vertex.

310 Taking all of these results together, each helix in an optimal tetrahelix is congruent to the
 311 others, shares an axis, is the same radius, and are evenly spaced axially. An optimal tetrahelix
 312 is therefore a *triple helix*, (of a radius we have not yet demonstrated.)

313 **4. Parameterizing Tetrahelices via Rail Angle.** We seek a formula to generate optimal
 314 tetrahelices that accepts a parameter that allows us to design the tetrahelix conveniently.
 315 Please refer back to [Figure 5](#). The pitch of the helix is an obvious choice, but is not defined
 316 when the curvature is 0, an important special case. The radius or the axial distance between
 317 two nodes on the same rail are possible choices, but perhaps the clearest choice is to build
 318 formulae that takes as their input the “rail angle” ρ . We define ρ to be the angle formed in
 319 the X,Y plane $\angle \mathbf{H}(0,0)O\mathbf{H}(0,1)$ projecting out the z axis and sighting along the positive z
 320 axis. In other words, ρ controls how far a rail edge of a tetrahelix deviates from being parallel
 321 with the axis, or the “twistiness” of the tetrahelix. We use the parameter $\chi = 1$ to indicate a
 322 chirality of counter-clockwise, and $\chi = -1$ for clockwise. We take our coordinate system to
 323 be right-handed.

324 The quantities ρ, r, d (see [Figure 5](#)) are related by the expression:

$$325 \quad 1^2 = d^2 + (2r \sin \rho/2)^2 \\ 326 \quad (6) \quad d^2 = 1 - 4r^2(\sin \rho/2)^2$$

327

329 Checking the important special case of the BC helix, we find that this equation indeed
 330 holds true (treating d in this equation as $3h_{bc}$ as defined by Gray and Coxeter, that is,
 331 $d_{bc} = 3h_{bc}$, where they are using h for the axial height from one node to the next of a different
 332 color, but we use d to mean distance between nodes of the same color.)

333 The rail angle ρ also has the meaning that $2\pi/\rho$ is the number of tetrahedra in a full
 334 revolution of the helix.

335 In choosing ρ , one greatly constrains r and d , but does not completely determine both of
 336 them together, so we treat both as additional parameters.

337 Rewriting our formulation in terms of ρ :

$$338 \quad (7) \quad \mathbf{H}_{general}(\chi, n, c, \rho, d_\rho, r_\rho) = \begin{bmatrix} r_\rho \cos(\chi \cdot (n\rho + c(\rho + 2\pi)/3)) \\ r_\rho \sin(\chi \cdot (n\rho + c(\rho + 2\pi)/3)) \\ d_\rho(n + c/3) \end{bmatrix}$$

339 where: $1 = d_\rho^2 + 4r_\rho^2(\sin \rho/2)^2$
 340 $\chi \in \{-1, 1\}$

341 $\mathbf{H}_{general}$ forces the user to select three values: ρ , r_ρ , and d_ρ satisfying (6).
 342 Note that when $\rho = 0$ then $d_\rho = 1$, but r_ρ is not determined by (6).

343 **Theorem 5.** For rail angles of magnitude at most ρ_{bc} , tetrahelices generated by $\mathbf{H}_{general}$
 344 are optimal in terms of minimum maximum ratio of member length when radius is chosen so
 345 that the length of the one-hop edge is equal to the rail length.

346 **Proof.** By Theorem 4, we can compute the (at most) three edge-lengths of an optimal
 347 tetrahelix by formula universally quantified by n and c :

$$348 \quad \text{rail} = \|\mathbf{H}_{general}(n, c, \rho, d_\rho, r) - \mathbf{H}_{general}(n+1, c, \rho, d_\rho, r)\| = 1$$

$$349 \quad \text{one-hop} = \|\mathbf{H}_{general}(n, c, \rho, d_\rho, r) - \mathbf{H}_{general}(n, c+1, \rho, d_\rho, r)\|$$

$$350 \quad \text{two-hop} = \|\mathbf{H}_{general}(n, c, \rho, d_\rho, r) - \mathbf{H}_{general}(n, c+2, \rho, d_\rho, r)\|$$

351

353 This syntax just represents the Euclidean distance formula.

$$354 \quad \text{one-hop} = \|\mathbf{H}_{general}(n, c, \rho, d_\rho) - \mathbf{H}_{general}(n, c+1, \rho, d_\rho), r\|$$

$$355 \quad \text{one-hop} = \sqrt{\frac{d_\rho^2}{9} + r^2(\sin^2(\rho/3 + \frac{2\pi}{3}) + (1 - \cos(\rho/3 + \frac{2\pi}{3}))^2)}$$

356 but: $d_\rho^2 = 1 - 4r^2(\sin(\rho/2)^2)$...so we substitute:

$$357 \quad \text{one-hop} = \sqrt{\frac{1}{9} + r^2(-\frac{4(\sin^2(\rho/2))}{9} + \sin^2(\rho/3 + \frac{2\pi}{3}) + (1 - \cos(\rho/3 + \frac{2\pi}{3}))^2)}$$

358

360 By similar algebra and trigonometry:

$$361 \quad \text{two-hop} = \sqrt{\frac{4}{9} + r^2(-\frac{16(\sin^2(\rho/2))}{9} + \sin^2(2\rho/3 + \frac{4\pi}{3}) + (1 - \cos(2\rho/3 + \frac{4\pi}{3}))^2)}$$

362

364 By definition of minimax edge length optimality, we are trying to minimize:

365

$$\frac{\max\{1, \text{one-hop}(r), \text{two-hop}(r)\}}{\min\{1, \text{one-hop}(r), \text{two-hop}(r)\}}$$

366 But since $\text{two-hop}(r) \geq \text{one-hop}(r)$, this is equivalent to:

367

$$\frac{\max\{1, \text{two-hop}(r)\}}{\min\{1, \text{one-hop}(r)\}}$$

368 This quantity will be equal to one of:

369 (8)
$$\frac{\text{two-hop}(r)}{1}, \frac{1}{\text{one-hop}(r)}, \frac{\text{two-hop}(r)}{\text{one-hop}(r)}$$

370 We know that both $\text{one-hop}(r)$ and $\text{two-hop}(r)$ increase monotonically and continuously
371 with increasing r . By inspection it seems likely that we will minimize this set by equating
372 $\text{one-hop}(r)$ or $\text{two-hop}(r)$ to 1, but to be absolutely sure and to decide which one, we must
373 examine the partial derivative of the ratio $\frac{\text{two-hop}(r)}{\text{one-hop}(r)}$ in this range.

374 Although complicated, we can use Mathematica to investigate the partial derivative of
375 the $\frac{\text{two-hop}(r)}{\text{one-hop}(r)}$ with respect to the radius to be able to understand how to choose the radius to
376 form the minimax optimum.

377 Let:

378

$$f_\rho = -\frac{4(\sin^2(\rho/2))}{9}$$

379

$$g_\rho = -\frac{16(\sin^2(\rho/2))}{9}$$

381

$$j_\rho = \sin^2(\rho/3 + \frac{2\pi}{3}) + (1 - \cos(\rho/3 + \frac{2\pi}{3}))^2$$

382

$$k_\rho = (\sin^2(2\rho/3 + \frac{4\pi}{3}) + (1 - \cos(2\rho/3 + \frac{4\pi}{3}))^2)$$

384 Then:

385

$$\frac{\text{two-hop}(r)}{\text{one-hop}(r)} = \frac{\sqrt{\frac{4}{9} + r^2(g_\rho + j_\rho)}}{\sqrt{\frac{1}{9} + r^2(f_\rho + k_\rho)}}$$

387 By graph inspection using Mathematica (<https://github.com/PubInv/tetrahelix/blob/master/tetrahelix.nb>), we see the partial derivative of this with respect to radius r is always
388 negative, for any $\rho \leq \rho_{bc}$. (When the rail angle approaches π , corresponding to going almost to
389 the other side of the tetrahelix, this is not necessarily true, hence the limitation in our state-
390 ment of the theorem is meaningful.) Since the partial derivative of $\text{two-hop}(r)/\text{one-hop}(r)$

392 with respect to the radius r is negative for all ρ up until ρ_{bc} , this ratio goes down as the radius
 393 goes up, and we minimize the maximum edge-length ratio by choosing the largest radius up
 394 until one-hop = 1, the rail-edge length. If we attempted to increase the radius further we
 395 would not be optimal, because the ratio $\frac{\text{two-hop}(r)}{1}$ would because the largest ratio in our set
 396 of ratios (8).

397 Therefore we decrease the minimax length of the whole system as we increase the radius
 398 up to the point that the shorter, one-hop distance is equal to the rail-length, 1. Therefore, to
 399 optimize the whole system so long as $\rho \leq \rho_{bc}$, we equate one-hop to 1 to find the optimum
 400 radius:

$$401 \quad 1 = \sqrt{\frac{1}{9} + r_{opt}^2 \left(-\frac{4(\sin^2(\rho/2))}{9} + \sin^2(\rho/3 + \frac{2\pi}{3}) + (1 - \cos(\rho/3 + \frac{2\pi}{3}))^2 \right)}$$

$$402 \quad (9) \quad r_{opt} = \frac{2}{\sqrt{\frac{9}{2} \cdot (\sqrt{3}\sin(\rho/3) + \cos(\rho/3)) + \cos(\rho) + 8}}$$

403

404 We can now give a formula for d_{opt} computed from ρ, r_{opt} via the rail angle equation (6):

$$406 \quad d_{opt}^2 = 1 - 4 \left(\frac{2}{\sqrt{\frac{9}{2} \cdot (\sqrt{3}\sin(\rho/3) + \cos(\rho/3)) + \cos(\rho) + 8}} \right)^2 (\sin \rho/2)^2$$

$$407 \quad d_{opt}^2 = 1 - \frac{16(\sin \rho/2)^2}{9(\sqrt{3}\sin(\rho/3) + \cos(\rho/3)) + \cos(\rho) + 8}$$

$$408 \quad (10) \quad d_{opt} = \sqrt{1 - \frac{16 \sin^2(\rho/2)}{\cos(\rho) + 9(\sqrt{3}\sin(\rho/3) + \cos(\rho/3)) + 8}}$$

409

410 Thus, by computing r_{opt} and d_{opt} as a function of ρ from this equation, we can construct
 411 minimax optimal tetrahelix for an $0 \leq \rho \leq \rho_{bc}$. ■

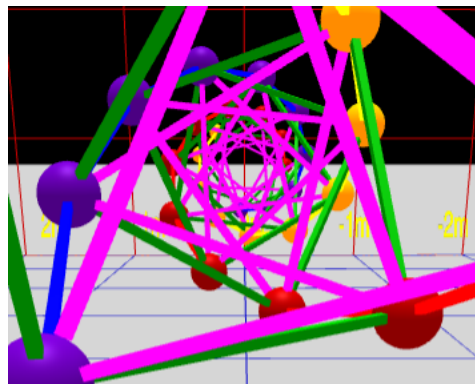


Figure 9. Axial view of a BC-Helix

5. The Inradius. Since the axes are parallel, we may define the *inradius*, represented by the letter i , of a tetrahelix to be the radius of the largest cylinder parallel to this axis that is surrounded by each tetrahelix and pentrated by no edge.

If we look down the axis of an optimal tetrahelix as shown in Figure 9, it happens that only the one-hop edges (rendered in purple in our software) comes closest to the axis. In other words, they define the radius of the incircle of the projection, or the radius of a cylinder that would just fit inside the tetrahelix. A formula for the inradius of the tetrahelix is useful if you are designing it as a structure that bears something internally, such as a firehose, a pipe, or a ladder for a human. The inradius $r_{in}(\rho)$ of an optimal tetrahelix is a remarkably simple function of the radius r and the rail angle ρ :

$$423 \quad (11) \qquad r_{in}(\rho) = r \sin \frac{\pi - \rho}{6}$$

424 Which can be seen from the trigonometry of a diagram of the projected one-hop edges con-
425 necting four sequentially numbered vertices:

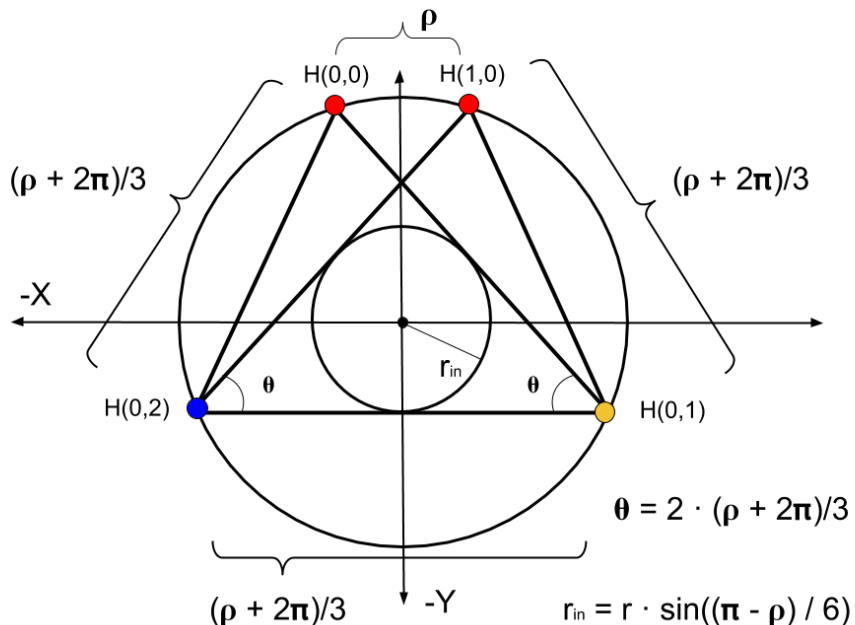


Figure 10. General One-hop Projection Diagram

From this equation with the help of symbolic computation we observe that inradius of the BC helix of unit rail length is $r_{in(\rho_{bc})} = \frac{3}{10\sqrt{2}} \approx 0.21$.

6. The Equitetrabeam. Just as $\mathbf{H}_{\text{general}}$ constructs the BC helix (with careful and non-obvious choices of parameters) which is an important special case due to its regularity, it constructs an additional special (degenerate) case when the rail angle $\rho = 0$ and $d = 1$ (the

431 edgelength), where the cross sectional area is an equilateral triangle of unchanging orientation,
 432 as shown in [Figure 8](#) and at the rear of [Figure 3](#). We call this the *equitetrabeam*. It is not
 433 possible to generate an equitetrabeam from [\(1\)](#) without the split into three rails introduced
 434 by [\(2\)](#) and completed in [\(7\)](#).

435 **Corollary 6.** *The equitetrabeam with minimal maximal edge ratio is produced*
 436 *by $\mathbf{H}_{\text{general}}$ when $r = \sqrt{\frac{8}{27}}$.*

437 **Proof.** Choosing $d = 1$ and $\rho = 0$ we use Equation [\(9\)](#) to find the radius of optimal
 438 minimax difference.

439 Substituting into [\(7\)](#):

$$440 \quad \text{one-hop} = \sqrt{\frac{1}{9} + 3r^2}$$

441

442 Then:

$$444 \quad 1 = \sqrt{\frac{1}{9} + 3r^2} \quad \text{solved by...}$$

$$445 \quad r = \sqrt{\frac{8}{27}} \quad \approx 0.54$$

446

447 This radius¹ produces a two-hop rail length of $\frac{2}{\sqrt{3}}$. The difference between this and 1 is
 448 $\approx 15.47\%$. The inradius of the equitetrabeam of unit rail length from both Equation [\(11\)](#) and
 449 the fact that the inradius of an equilateral triangle is half the circumradius is $\sqrt{\frac{8}{27}}/2$, or $\frac{\sqrt{6}}{9}$.

450 In [Figure 3](#), the furthest tetrahelix is the optimal equitetrabeam. [Figure 8](#) is a closeup of
 451 an equitetrabeam.

452 To the extent that we value tetrabeams (that is, tetrahelices with a rail angle of 0, and
 453 therefore zero curvature) as mathematical or engineering objects, we have motivated the
 454 development of $\mathbf{H}_{\text{general}}$ as a transformation of $\mathbf{V}(n)$ defined by Equation [\(1\)](#) from Gray and
 455 Coxeter. It is difficult to see how the $\mathbf{V}(n)$ formulation could ever give rise to a continuum
 456 producing the tetrabeam, since setting the angle in that equation to zero can produce only
 457 collinear points.

458 The equitetrabeam may possibly be a novel construction. The fact that 6 members meet
 459 in a single point would have been a manufacturing disadvantage that may have dissuaded
 460 structural engineers from using this geometry. However, the advent of additive manufacturing,
 461 such a 3D printing, and the invention of two distinct concentric multimember joints[\[15, 7\]](#) has
 462 improved that situation.

463 Note that the equitetrabeam has chirality, which becomes important in our attempt to
 464 build a continuum of tetrahelices.

¹Another interesting but non-optimal solution is derived by setting $(\text{one-hop} + \text{two-hop})/2 = 1$, occurs at $r = \sqrt{35}/4$ which produces three length classes of $11/12, 12/12, 13/12$.

466 **7. An Untwisted Continuum.** We observe that Equations (9) and (10) compute r_{opt}
 467 and d_{opt} which create an optimal tetrahelix for any rail angle ρ between 0, which gives the
 468 equitetrabeam and $\rho_{bc} \approx 35.43^\circ$, which gives the BC helix.

469 Because the equitetrabeam which has a rail angle of 0 still has chirality, that is, one still
 470 must decide to connect the one-hop edge to the clockwise or the counter-clockwise node, it is
 471 not possible to build a smooth continuum where ρ transitions from positive to negative which
 472 remains optimal. One can use a negative ρ in $\mathbf{H}_{general}$ but it does not produce minimax
 473 optimal tetrahelices. In other words, untwisting a counter-clockwise tetrahelix to rail angle 0
 474 and then going even further does produce a clockwise tetrahelix, but one in which the one-hop
 475 and two-hop lengths in the wrong places (that is, two-hop becomes shorter than one-hop.)
 476 Likewise, $\rho > \rho_{bc}$ generates a tetrahelix, but minimax optimality is not guaranteed by $\mathbf{H}_{general}$.

477 The pitch of a helix (see (4), for a fixed z -axis travel d , is trivial. However, if one is
 478 computing z -axis travel from (10) the pitch is not simple. It increases monotonically and
 479 smoothly with decreasing ρ , so Equation (4) can be easily solved numerically with a Newton-
 480 Raphson solver, as we do on our website. For a pitch at least $p \geq \frac{3\sqrt{2}\pi}{\sqrt{5}\rho_{bc}} \approx 9.64$, using (10)
 481 produces minimax optimal tetrahelices.

482 In this way a rail angle can be chosen for any desired (sufficiently large) pitch, yield the
 483 optimum radius, one-hop, and two-hop lengths an engineer needs to construct a physical
 484 structure.

485 The curvature of a rail helix is formally given by:

$$486 \quad (12) \quad \frac{|r_\rho|}{r_\rho^2 + (d_\rho/\rho)^2}$$

487 which goes to 0 as ρ approaches 0 (the equitetrabeam.) As ρ increase up to ρ_{bc} the curvature
 488 increases smoothly until the BC Helix is reached.

489 Perhaps surprisingly, the optimal untwisting is accomplished only by changing the length
 490 of the two-hop member, leaving the one-hop member and rail length equivalent within this
 491 continuum.² However, it should be noted that an engineer or architect may also use $\mathbf{H}_{general}$
 492 directly and interactively <https://pubinv.github.io/tetrahelix/>, and that minimax length opti-
 493 mality is a mathematical starting point rather than the final word on the beauty and utility of
 494 physical structures. For example, a structural engineer might increase radius past optimality
 495 in order to resist buckling.

496 If an equitetrabeam were actually used as a beam, an engineer might start with the
 497 optimal tetrabeam and dilate it in one dimension to “deepen” the beam. Similarly, simple
 498 length changes curve the equitetrabeam into an “arch”. The “colored” approach of (7) exposes
 499 these possibilities more than the approach of (1).

500 Trusses and space frames remain an important design field in mechanical and structural
 501 engineering[10], including deployable and moving trusses[2].

²Before deriving Equation (9), we created a continuum by using a linear interpolation between the optimal radius for the Equitetrabeam and the BC Helix. This minimax optimum of this simpler approach was at most 1% worse than the optimum computed by (9).

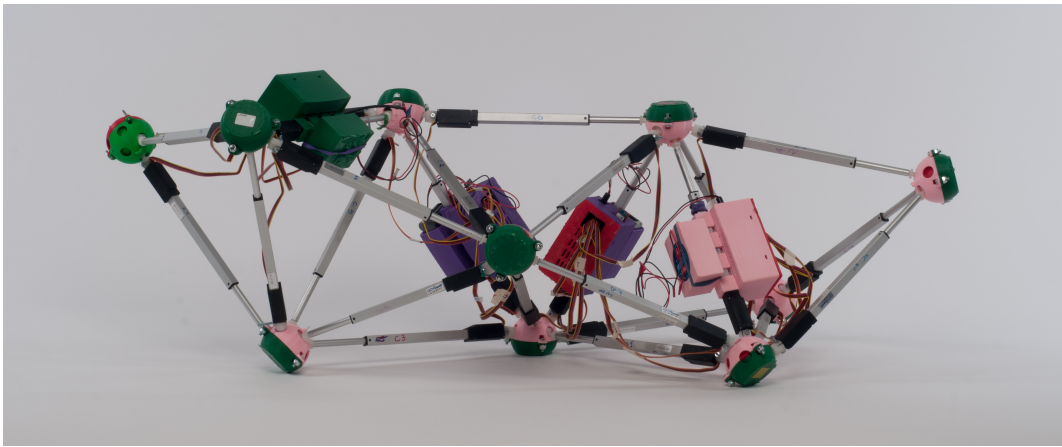


Figure 11. *Glussbot in relaxed, or BC helix configuration*

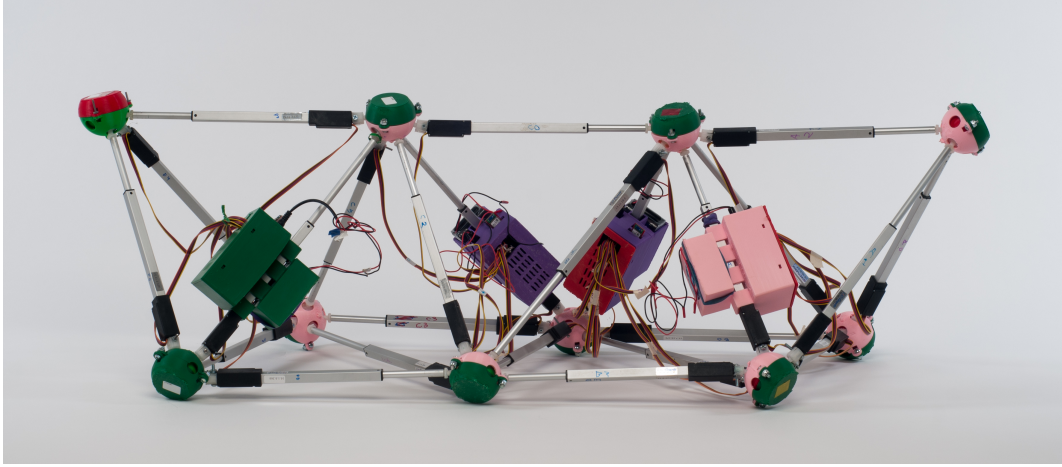


Figure 12. *The Equitetrabeam: Fully Untwisted Glussbot in Hexapod Configuration*

502 **8. Utility for Robotics.** Starting twenty years ago, Sanderson[14], Hamlin,[8], Lee[9], and
 503 others created a style of robotics based on changing the lengths of members joined at the
 504 center of a joint, thereby creating a connection to pure geometry. More recently NASA has
 505 experimented with tensegrities[1], a different point in the same design spectrum.

506 As suggested by Buckminster Fuller, the most convenient geometries to consider are those
 507 that have regular member lengths, in order to facilitate the inexpensive manufacture and
 508 construction of the robot. In a plane, the octet truss[4] is such a geometry, but in a line, the
 509 Boerdijk-Coxeter helix is a regular structure.

510 However, a robot must move, and so it is interesting to consider the transmutations of
 511 these geometries, which was in fact the motivation for creating the equitetrabeam.

512 **Theorem 7.** *By changing only the length of the longer members that connect two distinct
 513 rails (the two-hop members), we can dynamically untwist a glussbot forming the Boerdijk-
 514 Coxeter configuration into the equitetrabeam which rests flat on the plane.*

515 *Proof.* Proof by our computer program that does this using Equation (7) applied to the
516 7-tet Tetrobot/Glussbot.

517 By untwisting the tetrahelix so that it has a planar surface resting on the ground, we may
518 consider each vertex touching the ground a foot or pseudopod. A robot can thus become a
519 hexapod or n -pod robot, and the already well-developed approaches to hexapod gaits may be
520 applied to make the robot walk or crawl.

521 **9. Conclusion.** The BC Helix is the end point of a continuum of tetrahelices, the other end
522 point being an untwisted tetrahelix with equilateral cross section, constructed by changing the
523 length of only those members crossing the outside rails after hopping over the nearest vertex.
524 Under the condition of minimum maximum length ratios of all members in the system, all
525 such tetrahelices have vertices evenly spaced along the axis generated by a simple equation
526 and are in fact triple helices. A machine, such as a robot or a variable-geometry truss, that
527 can change the length of its members can thus twist and untwist itself by changing the length
528 of the appropriate members to achieve any point in the continuum. With a numeric solution,
529 a designer may choose a rotation angle and member lengths to obtain a desired pitch.

530 **10. Contact and Getting Involved.** The Gluss Project <http://pubinv.github.io/gluss/> is
531 part of Public Invention <https://pubinv.github.io/PubInv/>, a free-libre, open-source research,
532 hardware, and software project that welcomes volunteers. It is our goal to organize projects for
533 the benefit of all humanity without seeking profit or intellectual property. To assist, contact
534 read.robert@gmail.com.

535

REFERENCES

- 536 [1] *NTRT - NASA Tensegrity Robotics Toolkit.* <https://ti.arc.nasa.gov/tech/asr/intelligent-robotics/tensegrity/ntrt/>. Accessed: 2016-09-13.
- 537 [2] J. CLAYPOOL, *Readily configured and reconfigured structural trusses based on tetrahedrons as modules*,
538 Sept. 18 2012, <https://www.google.com/patents/US8266864>. US Patent 8,266,864.
- 539 [3] H. COXETER ET AL., *The simplicial helix and the equation $\tan(n \theta) = n \tan(\theta)$* , Canad. Math. Bull, 28
540 (1985), pp. 385–393.
- 541 [4] R. FULLER, *Synergetic building construction*, May 30 1961, <https://www.google.com/patents/US2986241>.
542 US Patent 2,986,241.
- 543 [5] R. FULLER AND E. APPLEWHITE, *Synergetics: explorations in the geometry of thinking*, Macmillan, 1982,
544 <https://books.google.com/books?id=G8baAAAAMAAJ>.
- 545 [6] R. W. GRAY, *Tetrahelix data*. <http://www.rwgrayprojects.com/rbfnotes/helix/helix01.html>, <http://www.rwgrayprojects.com/rbfnotes/helix/helix01.html> (accessed Accessed: 2017-04-08).
- 546 [7] G. J. HAMLIN AND A. C. SANDERSON, *A novel concentric multilink spherical joint with parallel robotics*
547 *applications*, in Proceedings of the 1994 IEEE International Conference on Robotics and Automation,
548 May 1994, pp. 1267–1272 vol.2, <https://doi.org/10.1109/ROBOT.1994.351313>.
- 549 [8] G. J. HAMLIN AND A. C. SANDERSON, *Tetrobot: A Modular Approach to Reconfigurable Parallel*
550 *Robotics*, Springer Science & Business Media, 2013, <https://play.google.com/store/books/details?id=izrSBwAAQBAJ> (accessed 2017-04-08).
- 551 [9] W. H. LEE AND A. C. SANDERSON, *Dynamic rolling locomotion and control of modular robots*, IEEE
552 Transactions on robotics and automation, 18 (2002), pp. 32–41.
- 553 [10] M. MIKULAS AND R. CRAWFORD, *Sequentially deployable maneuverable tetrahedral beam*, Dec. 10 1985,
554 <https://www.google.com/patents/US4557097>. US Patent 4,557,097.
- 555 [11] R. L. READ, *Gluss = Slug + Truss*. Unpublished preprint, <https://github.com/PubInv/gluss/blob/gh-pages/doc/Gluss.pdf> (accessed 2016-10-27).

- 560 [12] R. L. READ, *Untwisting the tetrahelix website*. <https://pubinv.github.io/tetrahelix/>, <https://pubinv.github.io/tetrahelix/> (accessed 2017-04-08).
- 561 [13] G. SADLER, F. FANG, J. KOVACS, AND K. IRWIN, *Periodic modification of the Boerdijk-Coxeter helix*
562 (*tetrahelix*), arXiv preprint arXiv:1302.1174, (2013), <https://arxiv.org/abs/1302.1174>.
- 563 [14] A. C. SANDERSON, *Modular robotics: Design and examples*, in Emerging Technologies and Factory Au-
564 tomation, 1996. EFTA'96. Proceedings., 1996 IEEE Conference on, vol. 2, IEEE, 1996, pp. 460–466.
- 565 [15] S. SONG, D. KWON, AND W. KIM, *Spherical joint for coupling three or more links together at one point*,
566 May 27 2003, <http://www.google.com/patents/US6568871>. US Patent 6,568,871.
- 567